Some optimised schemes for 1D Korteweg-de-Vries equation

A. R. Appadu[1], M. Chapwanya[2]& O. A. Jejeniwa[3]
[1,2,3] Department of Mathematics and Applied Mathematics, University of Pretoria,
Pretoria 0002, South Africa.
Corresponding author:[1] Email: rao.appadu@up.ac.za

Abstract

Two new explicit finite difference schemes for the solution of the one dimensional Korteweg-de-Vries equation are proposed. This equation describes the character of a wave generated by an incompressible fluid. We analyse the spectral properties of our schemes against two existing schemes proposed by Zabusky and Kruskal (*Phys. Rev. Lett.* 15(6):240–243,1965) and Wang *et al.* (*Chinese Phys. Lett.* 25(7):2335–2338, 2008). An optimization technique based on minimisation of the dispersion error is implemented to compute the optimal value of the spatial step size at a given value of the temporal step size and this is validated by some numerical experiments. The performance of the four methods are compared in regard to dispersive and dissipative errors and their ability to conserve mass, momentum and energy by using two numerical experiments which involve solitons.

Keywords: incompressible fluid, KdV, dissipation, dispersion, optimization, solitons.

Biographical notes: A. R. Appadu is currently a Senior Lecturer in the Department of Mathematics and Applied Mathematics at the university of Pretoria, South Africa. His current research interests are computational fluid dynamics, numerical analysis and numerical optimisation. He has about 25 publications in international journals and conference proceedings to date.

Dr Chapwanya is a Senior Lecturer in the Department of Mathematics and Applied Mathematics, University of Pretoria. His current research focus is in mathematical modelling, numerical analysis and scientific computation. The problems considered are drawn from a wide range of sources with biological, medical, engineering, industrial and environmental context.

O. A. Jejeniwa did his Bachelor and Master of Science degrees in the Department of Mathematics, Obafemi Awolowo University, Ile-Ife in Nigeria. He is currently a Ph.D student and an Assistant Lecturer in the Department of Mathematics and Applied Mathematics at the University of Pretoria, South Africa.

1 Introduction

In this work, we consider the generalized one dimensional Korteweg-de-Vries (KdV) equation in the form

$$u_t + \gamma u u_x + \beta u_{xxx} = 0, \quad x \in \mathbb{R}, \quad t > 0, \tag{1.1}$$

which describes the elongation of the wave generated by an incompressible fluid at position x and time t. Here α and β are positive constants. The second term in Eq. (1.1) shows non-linearity due to the occurrence of the product of the dependent variable and its derivative while the last term gives the order of the partial differential equation and is also responsible for dispersion. This equation which was first introduced by Korteweg and de Vries in [1] depicts the character of shallow incompressible fluid waves with small but finite amplitudes. Ludu *et al* [2] generalized the non-linear one-dimensional equation of a fluid layer for any depth and length as an infinite order differential equation for steady waves, and in the limit of long and shallow incompressible fluid (shallow channel), they reobtained the well known KdV equation together

with its single soliton solution. It has been used to describe the occurrences of waves in bubble-liquid mixtures (incompressible fluid mixture) [3, 4], anharmonic crystals [5, 6] and plasma physics [7, 8]. The equation is also important in the analysis of the interaction between nonlinearity and dispersion, as seen in the well-known Burgers equation which displays the properties of the interaction between nonlinearity and dissipation [9]. The integrability of (1.1) guaranties an infinite invariants. These quantities are constant along the solution of the given partial differential equation [10], and here we state the first three invariants as follows:

$$\begin{aligned} F_1(u) &= \int_{\mathbb{R}} u \, dx, \\ F_2(u) &= \frac{1}{2}\int_{\mathbb{R}} u^2 \, dx, \\ F_3(u) &= \int_{\mathbb{R}} \left(\frac{\beta}{2}u_x^2 - \frac{\gamma}{6}u^3\right) dx. \end{aligned} \tag{1.2}$$

which represent the mass, momentum and energy conservation respectively.

A lot of effort has been devoted to the design of stable, efficient and reliable numerical schemes for the KdV equation. The most well known explicit finite difference scheme for (1.1) was proposed by Zabusky and Kruskal [11] where the time derivative is leap-frog like in nature. The scheme is second order in time and conserves the first integral in (1.2) to a high degree of accuracy (see for example [10]). A method which involves the use of central difference for space derivatives together with a predictor corrector time step was proposed by [12]. The method was analyzed based on stability criteria and numerical dispersion. Numerical experiments for the single soliton and for the interaction of more than one soliton were presented graphically.

Ascher and McLachlan [13] gave an account of the study of symplectic and multi-symplectic schemes for the KdV equation in order to answer the question of whether added structure preservation such as conservative discretization schemes would provide high quality schemes for long time integration of nonlinear conservative PDEs. KdV equation was used as a case study, they concluded that it is possible to design a very stable, conservative difference schemes for the nonlinear, conservative KdV equation. In 2005, Refik [14] used an exponential finite difference scheme, a method developed by Bhattacharya [15], to solve the KdV equation. It was concluded that the method generates numerical results of KdV equation which are accurate for small time steps. Recently, Wang et al. [10] proposed a scheme (W-W-H scheme) which was obtained by substituting an average of forward and backward difference in time in place of central difference in time in Z-K scheme. They carried out numerical simulations of KdV equation with initial condition $u(x, 0) = \cos x$ and it was found that their scheme did not blow up at a longer time when compared with Zabusky and Kruskal scheme and multi-symplectic six-point scheme. They also showed that their scheme has more relaxed stability than Zabusky and Kruskal scheme and multi-symplectic six-point scheme. Attention of many researchers have been drawn towards studying this equation due to the importance as benchmark for proposed schemes, or to reproduce the qualitative behavior of the solutions of the equation as above, but no attention has been paid to the optimization of the methods used in solving this equation. In this work, we obtain expressions for the amplification factor and the region of stability for the schemes considered. We also obtain relative phase error for the schemes and then optimized the schemes to compute the optimal value of the spatial step size at a given value of the temporal step size. Similar analysis can also be carried out on higher order schemes.

This paper is organised as follows. Section 2 introduces two existing numerical schemes and also presents the regions of stability of the schemes. In Section 3, the dissipative and dispersive properties of the schemes are presented and analytical expressions for their relative phase error are obtained. In Section 4, we quantify errors from the numerical results into dissipation and dispersion errors by using a technique devised by Takacs [16] and obtain some errors based on conservation laws for the equation. In Section 5,

two additional schemes are introduced, results obtained using the four schemes are presented graphically, we also tabulate the errors for the methods used in solving the numerical experiments described. In Section 6, we find the optimal value for the spatial grid size for a fixed value of the time step for the four schemes. Numerical experiments are presented throughout to validate these results. Section 7 contains the conclusions and possible future work.

2 Numerical schemes for KdV equation

In this section we describe two existing schemes, the first scheme was introduced in [11] and the second scheme in [10]. We will investigate the stability of each of the presented scheme for $\gamma = 6$, $\beta = 1$. From now onwards, our study will be based on the partial differential equation

$$u_t + 6uu_x + u_{xxx} = 0, \quad x \in \mathbb{R}, \quad t > 0. \tag{2.1}$$

The equation is solved on a truncated domain with a uniform mesh $h > 0$, and spatial node, $x_m = mh$, $m = 0, 1, \cdots, N$. The time node is given by $t_n = nk$ where $k > 0$ is the step size and $n = 0, 1, \cdots$. The exact value of the solution at (t_n, x_m) is denoted by $u(t_n, x_m)$ while the discrete numerical solution is denoted by u_m^n.

2.1 Zabusky and Kruskal scheme (1965)

The scheme uses central difference approximations in both space and time and is given by

$$\frac{u_m^{n+1} - u_m^{n-1}}{2k} + 6\left(\frac{u_{m+1}^n + u_m^n + u_{m-1}^n}{3}\right)\left(\frac{u_{m+1}^n - u_{m-1}^n}{2h}\right) + \left(\frac{u_{m+2}^n - 2u_{m+1}^n + 2u_{m-1}^n - u_{m-2}^n}{2h^3}\right) = 0, \tag{2.2}$$

which can be written explicitly as

$$u_m^{n+1} = u_m^{n-1} - 2\lambda\left(u_{m+1}^n + u_m^n + u_{m-1}^n\right)\left(u_{m+1}^n - u_{m-1}^n\right) - \frac{\lambda}{h^2}\left(u_{m+2}^n - 2u_{m+1}^n + 2u_{m-1}^n - u_{m-2}^n\right), \tag{2.3}$$

where $\lambda = k/h$ is the Courant-Friedrichs-Lewy (CFL) number. This scheme is consistent of order two in both space and time. On $\mathbb{R}$, the stability region is obtained by method of freezing of coefficients [17] and application of Von Neumann stability analysis i.e., we express uu_x as $u_{\max}u_x$ and substitute the ansatz $u_m^n = \xi^n e^{Im\omega}$, where $\omega = \theta h$, to obtain the amplification factor

$$\xi^2 + I\left\{12\lambda u_{\max}\sin\omega + \frac{\lambda}{h^2}\left(2\sin 2\omega - 4\sin\omega\right)\right\}\xi - 1 = 0, \tag{2.4}$$

where ξ is the amplification factor, θ is the wave number, ω is the phase angle and $I = \sqrt{-1}$. Eq. (2.4) can be written as

$$A\xi^2 + B\xi + C = 0,$$

where

$$A = 1, \quad B = I\left\{12\lambda u_{\max}\sin\omega + \frac{\lambda}{h^2}\left(2\sin 2\omega - 4\sin\omega\right)\right\} \quad \text{and} \quad C = -1.$$

For stability, we follow the analysis in [18, 19]. In particular, we let

$$f(\xi) = A\xi^2 + B\xi + C,$$

and suppose $\xi^* = \frac{1}{\xi}$, then

$$f(\xi^*) = A\bar{\xi}^{-2} + B\bar{\xi}^{-1} + C,$$

and

$$f(\bar{\xi}^*) = \bar{A}\xi^{-2} + \bar{B}\xi^{-1} + \bar{C},$$

therefore with $f^*(\xi) = \xi^2 f(\bar{\xi}^*)$, we have

$$f^*(\xi) = \bar{A} + \bar{B}\xi + \bar{C}\xi^2,$$

where

$$\bar{A} = 1, \quad \bar{B} = -I\left\{12\lambda u_{\max}\sin\omega + \frac{\lambda}{h^2}(2\sin 2\omega - 4\sin\omega)\right\} \quad \text{and} \quad \bar{C} = -1.$$

We define the Bezout resultant as

$$\tilde{f} = \frac{1}{\xi}[f^*(0)f(\xi) - f(0)f^*(\xi)] = (A\bar{A} - C\bar{C})\xi + (\bar{A}B - \bar{B}C), \tag{2.5}$$

where $f^*(0) = \bar{A}$ and $f(0) = C$. For f to be von Neumann, we must show that $\tilde{f} \equiv 0$ and $f^{'}(\xi)$ is Von Neumann. On substituting the values of A, $\bar{A}$, B, $\bar{B}$, C and $\bar{C}$ into Eq. (2.5), we have $\tilde{f} \equiv 0$. Then, for f to be von Neumann, we are required to show that $f^{'}(\xi) = 2A\xi + B$ is von Neumann. Hence, we require that $|\xi| \leq 1$ for this function, i.e.,

$$|\xi| = \left|\frac{-B}{2A}\right| \leq 1.$$

On substituting the values of A and B, we have

$$\left|-I\left\{12\lambda u_{\max}\sin\omega + \frac{\lambda}{h^2}(2\sin 2\omega - 4\sin\omega)\right\}\right| \leq 2.$$

Since the second expression in the bracket for the above inequality dominates the first for small values of h, we obtain $\omega = 2\pi/3$ from the second expression which gives the maximum value for the inequality. On substituting this into the inequality, we obtain the region of stability as

$$\lambda \leq \left|\frac{2}{3\sqrt{3}(2u_{\max} - \frac{1}{h^2})}\right|, \tag{2.6}$$

where $u_{\max}$ is the maximum value of u.

2.2 Wang et al. scheme (2008)

The second scheme considered here and first derived in [10] was inspired by the Z-K scheme introduced above, it is denoted by W-W-H scheme. Here the time derivative is replaced by an average of the forward difference approximation at grid point $m-1$ and backward difference approximation at grid point $m+1$ while the space derivative is replaced by central difference approximation. The W-W-H scheme is given by

$$\frac{1}{2}\left(\frac{u_{m-1}^{n+1} - u_{m-1}^{n}}{k} + \frac{u_{m+1}^{n} - u_{m+1}^{n-1}}{k}\right) + 6\left(\frac{u_{m+1}^{n} + u_{m}^{n} + u_{m-1}^{n}}{3}\right)\left(\frac{u_{m+1}^{n} - u_{m-1}^{n}}{2h}\right) + \left(\frac{u_{m+2}^{n} - 2u_{m+1}^{n} + 2u_{m-1}^{n} - u_{m-2}^{n}}{2h^3}\right) = 0, \tag{2.7}$$

which, for implementation, can be written as

$$u_{m-1}^{n+1} = u_{m-1}^{n} - u_{m+1}^{n} + u_{m+1}^{n-1} - 2\lambda\left(u_{m+1}^{n} + u_{m}^{n} + u_{m-1}^{n}\right)\left(u_{m+1}^{n} - u_{m-1}^{n}\right) - \frac{\lambda}{h^2}\left(u_{m+2}^{n} - 2u_{m+1}^{n} + 2u_{m-1}^{n} - u_{m-2}^{n}\right), \tag{2.8}$$

which is a consistent scheme of order two in both space and time. As before, we initialize the simulations using Eq. (5.1). Similarly, by method of freezing of coefficients and application of Von Neumann stability analysis, the amplification factor is given below as

$$(\cos\omega - I\sin\omega)\xi^2 + 2I\sin\omega\left(1 + 6\lambda u_{\max} + 2\frac{\lambda}{h^2}(\cos\omega - 1)\right)\xi - (\cos\omega + I\sin\omega) = 0. \tag{2.9}$$

This can be written as

$$A\xi^2 + B\xi + C = 0,$$

where

$$A = \cos\omega - I\sin\omega, \quad B = 2I\sin\omega\left(1 + 6\lambda u_{\max} + 2\frac{\lambda}{h^2}(\cos\omega - 1)\right) \quad \text{and} \quad C = -(\cos\omega + I\sin\omega).$$

Following the same analysis as in subsection (2.1), we obtain the region of stability given below as

$$\left|1 + 3\lambda\left\{2u_{\max} - \frac{1}{h^2}\right\}\right| \leq \frac{2}{\sqrt{3}}. \tag{2.10}$$

3 Numerical Dispersion

The consistent reduction with time, of the amplitude of plane waves is called dissipation. Dissipative schemes suppress high frequency waves that can cause numerical solutions to be more oscillatory than required [17]. Dispersion is an occurrence of waves of different frequencies traveling at different speeds. It causes numerical solutions to spread out as time advances. Our KdV equation is dispersive in nature as a result of the third order derivative term. Relative phase error (RPE), is defined as the ratio of the numerical phase velocity to the exact phase velocity. If the ratio is greater than unity, then the computed waves move faster than the exact waves, thereby causing phase lead. Phase lag occurs when the computed waves move slower than the exact waves.
Ascher and McLachlan [13] have obtained the dispersion relation of the partial differential equation,

$$u_t = 2\zeta u u_x + \rho u_x + \nu u_{xxx}, \tag{3.1}$$

by considering the linearized version of Eq. (3.1) in the form

$$u_t = \rho u_x + \nu u_{xxx}. \tag{3.2}$$

When discretized by the Z-K scheme, Eq. (3.2) gives

$$u_m^{n+1} = u_m^{n-1} + \rho\lambda(u_{m+1}^{n} - u_{m-1}^{n}) + \frac{\nu\lambda}{h^2}(u_{m+2}^{n} - 2u_{m+1}^{n} + 2u_{m-1}^{n} + u_{m-2}^{n}). \tag{3.3}$$

They considered plane wave solutions of the form

$$u_m^n = \exp\left(I[\omega m + \Omega^* n]\right) = \exp\left(I\left[\frac{\omega}{h}mh + \frac{\Omega^*}{k}nk\right]\right), \tag{3.4}$$

where Ω^* is the numerical dispersion relation and

$$u(x,t) = \exp\left(I\left[\frac{\omega}{h}x + \frac{\Omega}{k}t\right]\right), \tag{3.5}$$

where Ω is the dispersion relation and ω is the phase angle. Using Eq. (3.5) and (3.2), we obtain the exact dispersion relation given by

$$\Omega = k\rho\frac{\omega}{h} - k\nu\left(\frac{\omega}{h}\right)^3,$$

which can be written as

$$\Omega = k\rho\theta - k\nu\theta^3,$$

since $w = \theta h$. On the other hand, the numerical dispersion relation for Z-K scheme for Eq. (3.2) satisfies the equation

$$e^{I\Omega^*} = e^{-I\Omega^*} + \rho\lambda(e^{I\omega} - e^{-I\omega}) + \frac{\nu\lambda}{h^2}(e^{2I\omega} - 2e^{I\omega} + 2e^{-I\omega} + e^{-2I\omega}),$$

which simplifies as

$$\Omega^* = \sin^{-1}\left(\rho\lambda\sin\theta h + \frac{\nu\lambda}{h^2}(\sin 2\theta h - 2\sin\theta h)\right).$$

Following the same idea as Ascher and Mc Lachlan, we obtain the linearized version of Eq. (2.1) which is

$$u_t + u_{xxx} = 0, \tag{3.6}$$

we then obtain expressions for the relative phase error of the two schemes when used to discretise Eq. (3.6).

When Zabusky and Kruskal (1965) scheme is used to approximate Eq. (3.6), we have

$$u_m^{n+1} = u_m^{n-1} - \frac{\lambda}{h^2}\left(u_{m+2}^n - 2u_{m+1}^n + 2u_{m-1}^n - u_{m-2}^n\right). \tag{3.7}$$

Let elementary solution of Eq. (3.6) be

$$u(x,t) = e^{I\theta x}e^{\alpha t},$$

see [20]. Then $u_t = \alpha e^{\alpha t}e^{I\theta x}$, $u_x = I\theta e^{I\theta x}e^{\alpha t}$, $u_{xx} = (I\theta)^2 e^{I\theta x}e^{\alpha t}$ and $u_{xxx} = (I\theta)^3 e^{I\theta x}e^{\alpha t}$. Substituting these into Eq. (3.6) and simplifying, we get

$$\alpha + (I\theta)^3 = 0,$$

which gives $\alpha = I\theta^3$. Hence,

$$u(x,t) = e^{I\theta x}e^{I\theta^3 t} = e^{I\theta x}a(t),$$

where $a(t) = e^{I\theta^3 t}$.

The amplification factor is calculated as

$$\xi_{exact} = \frac{a(t^{n+1})}{a(t^n)} = \frac{e^{Ik\theta^3(n+1)}}{e^{Ik\theta^3(n)}},$$

and on simplifying, we have

$$\xi_{exact} = e^{Ik\theta^3},$$

where $|\xi_{exact}| = 1$ since the PDE is not dissipative. ξ_{num} is obtained from Von Neumann stability analysis. The relative phase error is given by [21]

$$RPE = \frac{\arg(\xi_{num})}{\arg(\xi_{exact})},$$

where

$$\xi_{exact} = \cos(k\theta^3) + I\sin(k\theta^3),$$

therefore,

$$\arg(\xi_{exact}) = \tan^{-1}\left(\frac{\sin(k\theta^3)}{\cos(k\theta^3)}\right) = k\theta^3.$$

We let

$$\xi_{num} = \xi_1 + I\xi_2,$$

where ξ_1 and ξ_2 are the real and imaginary parts of ξ_{num}, then

$$\arg(\xi_{num}) = \tan^{-1}\left(\frac{\xi_2}{\xi_1}\right),$$

therefore

$$\text{RPE} = \frac{1}{k\theta^3}\tan^{-1}\left(\frac{\xi_2}{\xi_1}\right).$$

Using $\theta = \omega/h$ we have

$$\text{RPE} = \frac{h^3}{k\omega^3}\tan^{-1}\left(\frac{\xi_2}{\xi_1}\right).$$

To obtain the amplification factor for Z-K scheme, we substitute $u_m^n = \xi^n e^{I\theta mh}$ into Eq. (3.7) and simplify to obtain

$$\xi = \sqrt{1 - \frac{\lambda^2}{h^4}(\sin 2\theta h - 2\sin\theta h)^2} + I\left\{\frac{\lambda}{h^2}(2\sin\theta h - \sin 2\theta h)\right\}. \tag{3.8}$$

Hence,

$$\text{RPE} = \frac{h^2}{\lambda\omega^3}\tan^{-1}\left\{\frac{\frac{\lambda}{h^2}(2\sin\omega - \sin 2\omega)}{\sqrt{1 - \frac{\lambda^2}{h^4}(\sin 2\omega - 2\sin\omega)^2}}\right\}.$$

When the Wang *et* al. (1998) Scheme is used to approximate Eq. (3.6), we have

$$u_{m-1}^{n+1} = u_{m-1}^n - u_{m+1}^n + u_{m+1}^{n-1} - \frac{\lambda}{h^2}\left(u_{m+2}^n - 2u_{m+1}^n + 2u_{m-1}^n - u_{m-2}^n\right). \tag{3.9}$$

On substituting $u_m^n = \xi^n e^{I\theta mh}$ into Eq. (3.9) and simplifying, we obtain

$$\xi_{num} = \left(\frac{-P\sin\omega + Q\cos\omega}{2}\right) + I\left(\frac{P\cos\omega + Q\sin\omega}{2}\right), \tag{3.10}$$

where

$$P = -2\sin\omega\left\{1 + 2\frac{k}{h^3}(\cos\omega - 1)\right\} \tag{3.11}$$

and

$$Q = 2\sqrt{1 - \sin^2\omega\left\{1 + 2\frac{k}{h^3}(\cos\omega - 1)\right\}^2}. \tag{3.12}$$

The corresponding expression for the relative phase error of the W-W-H scheme is given by

$$\text{RPE} = \frac{h^2}{\lambda\omega^3}\tan^{-1}\left\{\frac{P\cos\omega + Q\sin\omega}{Q\cos\omega - P\sin\omega}\right\}.$$

Plots of the relative phase error versus phase angle at different values of h when $k = 0.001$ and $k = 0.0015$ are shown in Figs. 1 and 2. For small values of phase angle, at a given value of k, the relative phase error is not much affected by changes in the values of h for Z-K scheme. In the case of W-W-H scheme, changes in the values of h affect the relative phase error more.

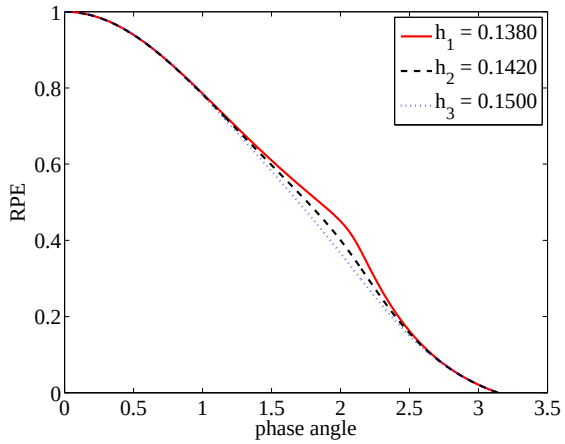

(a) Profiles for $k = 0.001$.

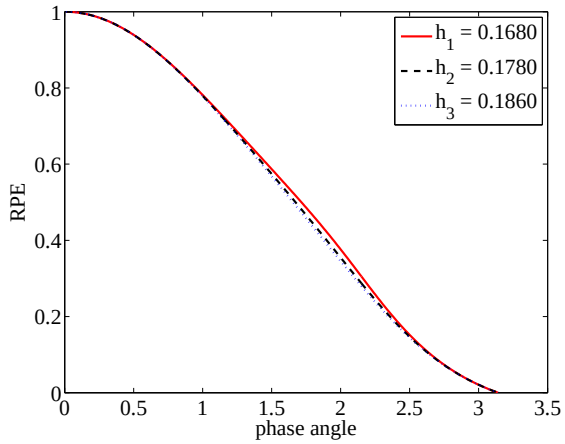

(b) Profiles for $k = 0.0015$.

Figure 1: Plot of relative phase error versus phase angle for Z-K scheme. The same profiles can be used for the new proposed schemes.

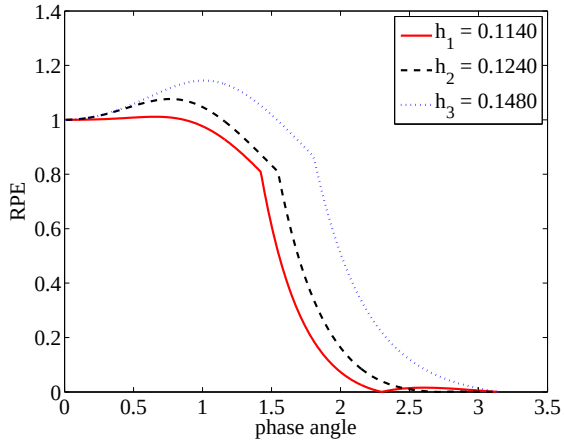

(a) Profiles for $k = 0.001$.

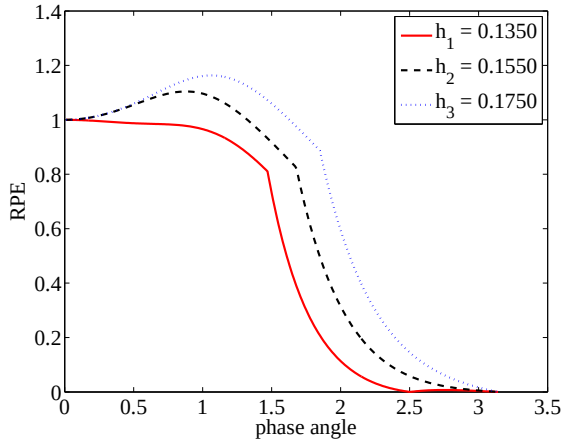

(b) Profiles for $k = 0.0015$.

Figure 2: Plot of relative phase error versus phase angle for W-W-H scheme.

4 Quantification of errors and conservation laws

Takacs [16] quantifies the errors from numerical results into dispersion and dissipation errors. Many interesting applications using the technique of Takacs can be seen in [22, 23, 24, 25]. In this section, we use the ideas from [16] to quantify errors from numerical results into dissipation and dispersion. We also look at the conservation laws of Eq. (2.1) under periodic boundary conditions.

4.1 Dispersion and dissipation errors

We begin by defining the Total Mean Square Error (TMSE) [16], as

$$\frac{1}{N}\sum_{m=1}^{N}(u_m - v_m)^2, \tag{4.1}$$

where u_m and v_m are the analytical and numerical solutions respectively, at a given grid point m and time t. We can write the TMSE as

$$\frac{1}{N}\sum_{m=1}^{N}(u_m - v_m)^2 = \frac{1}{N}\sum_{m=1}^{N}(u_m)^2 + \frac{1}{N}\sum_{m=1}^{N}(v_m)^2 - \frac{2}{N}\sum_{m=1}^{N} u_m v_m. \tag{4.2}$$

Let $\bar{u}$ and $\bar{v}$ be the mean values of u_m and v_m respectively. Using the definition of variance, we can also write

$$\frac{1}{N}\sum_{m=1}^{N}(u_m - \bar{u})^2 = \frac{1}{N}\sum_{m=1}^{N}(u_m^2 - 2u_m\bar{u} + \bar{u}^2), \tag{4.3}$$

$$\frac{1}{N}\sum_{m=1}^{N}(v_m - \bar{v})^2 = \frac{1}{N}\sum_{m=1}^{N}(v_m^2 - 2v_m\bar{v} + \bar{v}^2). \tag{4.4}$$

The TMSE can therefore be written as

$$\begin{aligned}\frac{1}{N}\sum_{m=1}^{N}(u_m - \bar{u})^2 + \frac{1}{N}\sum_{m=1}^{N}(v_m - \bar{v})^2 + \frac{2}{N}\sum_{m=1}^{N} u_m\bar{u} + \frac{2}{N}\sum_{m=1}^{N} v_m\bar{v} \\ -\frac{1}{N}\sum_{m=1}^{N}\bar{u}^2 - \frac{1}{N}\sum_{m=1}^{N}\bar{v}^2 - \frac{2}{N}\sum_{m=1}^{N} u_m v_m.\end{aligned} \tag{4.5}$$

The expression in Eq.(4.5) can be written as

$$\sigma^2(u) + \sigma^2(v) + 2\bar{u}^2 + 2\bar{v}^2 - \bar{u}^2 - \bar{v}^2 - \frac{2}{N}\sum_{m=1}^{N} u_m v_m, \tag{4.6}$$

where $\sigma^2(u)$ and $\sigma^2(v)$ represent the variance of u and v respectively, $\bar{u}$ and $\bar{v}$ denote the mean values of u and v respectively. Therefore the TMSE is given by

$$\sigma^2(u) + \sigma^2(v) + (\bar{u}^2 - 2(\bar{u})(\bar{v}) + \bar{v}^2) + \left(2(\bar{u})(\bar{v}) - \frac{2}{N}\sum_{m=1}^{N} u_m v_m\right), \tag{4.7}$$

which further simplifies to

$$\sigma^2(u) + \sigma^2(v) + (\bar{u} - \bar{v})^2 - 2\left(\frac{1}{N}\sum_{m=1}^{N} u_m v_m - (\bar{u})(\bar{v})\right), \tag{4.8}$$

therefore, we have

$$\frac{1}{N}\sum_{m=1}^{N}(u_m - v_m)^2 = \sigma^2(u) + \sigma^2(v) + (\bar{u} - \bar{v})^2 - 2\,Cov(u, v). \tag{4.9}$$

Since the correlation coefficient, ρ, is given by the fraction $\frac{Cov(u,v)}{\sigma(u)\sigma(v)}$, the TMSE is therefore written as

$$\frac{1}{N}\sum_{m=1}^{N}(u_m - v_m)^2 = \sigma^2(u) + \sigma^2(v) + (\bar{u} - \bar{v})^2 - 2\,\rho\,\sigma(u)\,\sigma(v), \tag{4.10}$$

which reduces to

$$\frac{1}{N}\sum_{m=1}^{N}(u_m - v_m)^2 = (\sigma(u) - \sigma(v))^2 + (\bar{u} - \bar{v})^2 + 2\,(1-\rho)\,\sigma(u)\,\sigma(v). \tag{4.11}$$

On setting $\rho = 1$, we obtain $2\,(1-\rho)\,\sigma(u)\,\sigma(v) = 0$. Thus, we define $2(1-\rho)\sigma(u)\sigma(v)$ as the dispersion error as correlation coefficient in Statistics, is analogous to phase lag or phase lead in Computational Fluid Dynamics. Hence, $(\sigma(u)-\sigma(v))^2 + (\bar{u}-\bar{v})^2$ measures the dissipation error, N being the number of spatial grid points.

4.2 Conservation Laws

The discrete forms of the three conservation laws in Eq. (1.2) are given as [10]

$$F_1^h(\mathbf{u}) = \sum_{m=1}^{N} u_m h, \tag{4.12}$$

$$F_2^h(\mathbf{u}) = \frac{1}{2}\sum_{m=1}^{N}\left(\frac{u_m + u_{m-1}}{2}\right)^2 h, \tag{4.13}$$

$$F_3^h(\mathbf{u}) = \sum_{m=1}^{N}\left\{\frac{1}{2}|\triangle_+ u_m|^2 - \frac{1}{6}u_m^3\right\} h, \tag{4.14}$$

where F_1, F_2 and F_3 are the mass, momentum and energy respectively and $\Delta_+ u_m = (u_{m+1} - u_{m-1})/2h$. We shall fix k to compute the errors in conservation laws for the three schemes using

$$\text{error } F_1 = F_1^h(\mathbf{u}^n) - F_1^h(\mathbf{u}^0), \tag{4.15}$$

$$\text{error } F_2 = F_2^h(\mathbf{u}^n) - F_2^h(\mathbf{u}^0), \tag{4.16}$$

$$\text{error } F_3 = F_3^h(\mathbf{u}^n) - F_3^h(\mathbf{u}^0), \tag{4.17}$$

where $\mathbf{u}^n$ is the numerical solution at the n^{th} time level and $\mathbf{u}^0$ is the discrete initial time solution.

5 Numerical experiments

In this section, we present several numerical simulations for equation (2.1) subject to specified initial and boundary conditions using the two existing schemes introduced in Section 2, and then introduce our proposed schemes. For implementation, we initialize the time steps using the following forward difference in time scheme

$$u_m^1 = u_m^0 - \lambda(u_{m+1}^0 + u_m^0 + u_{m-1}^0)\left(u_{m+1}^0 - u_{m-1}^0\right) - \frac{\lambda}{2h^2}\left(u_{m+2}^0 - 2u_{m+1}^0 + 2u_{m-1}^0 - u_{m-2}^0\right). \tag{5.1}$$

We begin by considering the single soliton problem

Experiment 1

$$\begin{cases} u_t + 6uu_x + u_{xxx} = 0, \ \ \forall\,(x,t) \in (-L,L)\times(0,T), \\ u(x,0) = v(x,0)\,, \\ u(x-L,t) = u(x+L,t). \end{cases} \tag{5.2}$$

where $L = 20$ and $v(x,t)$ is the exact solution given by

$$v(x,t) = \frac{2\mu^2}{\cosh^2[\mu(x - 4\mu^2 t)]}.$$

See [26]

Experiment 1 represents a wave packet with amplitude $2\mu^2$ and wave velocity $4\mu^2$. In all the simulations, we choose $T = 3$, $T = 6$ and $\mu = 1/\sqrt{2}$.

From the stability analysis of the Z-K scheme, with $k = 0.0010$ and $k = 0.0015$, the respective regions of stability satisfy the inequalities: $h \geq 0.1358$ and $h \geq 0.1548$. We tabulate the dissipation, dispersion and TMSE in Table 1 and observe that the dispersion error is much greater than the dissipation error. We also observe that the dispersion error is least when $h = 0.1574$ and greatest when $h = 0.1860$ for $k = 0.0015$.

Table 1: Errors for the schemes at $T = 3$ when $k = 0.0015$ for 1-soliton experiment.

Schemes	h	Dissipation error	Dispersion error	TMSE
Scheme (2.2) Z-K	0.1574	1.0951×10^{-13}	4.6514×10^{-6}	4.6514×10^{-6}
	0.1680	2.3375×10^{-13}	6.1566×10^{-6}	6.1566×10^{-6}
	0.1780	8.2518×10^{-13}	9.2490×10^{-6}	9.2490×10^{-6}
	0.1860	7.2674×10^{-13}	9.4603×10^{-6}	9.4603×10^{-6}
Scheme (2.7) W-W-H	0.1289	6.7403×10^{-11}	2.3402×10^{-5}	2.3402×10^{-5}
	0.1350	9.8285×10^{-11}	2.8137×10^{-5}	2.8137×10^{-5}
	0.1550	3.4079×10^{-10}	4.8620×10^{-5}	4.8621×10^{-5}
	0.1650	4.7927×10^{-10}	6.3868×10^{-5}	6.3868×10^{-5}
Scheme (5.3) NS1	0.1574	6.5719×10^{-12}	1.4464×10^{-5}	1.4464×10^{-5}
	0.1680	1.1141×10^{-11}	1.9062×10^{-5}	1.9062×10^{-5}
	0.1780	3.8082×10^{-11}	2.7082×10^{-5}	2.7082×10^{-5}
	0.1860	2.6184×10^{-11}	2.9164×10^{-5}	2.9164×10^{-5}
Scheme (5.4) NS2	0.1574	1.9474×10^{-13}	6.5337×10^{-6}	6.5337×10^{-6}
	0.1680	4.4682×10^{-13}	8.6368×10^{-6}	8.6368×10^{-6}
	0.1780	1.8065×10^{-12}	1.2761×10^{-5}	1.2761×10^{-5}
	0.1860	1.2850×10^{-12}	1.3250×10^{-5}	1.3250×10^{-5}

The respective regions of stability for the W-W-H scheme satisfy the inequalities: $h \geq 0.11074$ and $h \geq 0.12645$ as obtained from the stability analysis for $k = 0.0010$ and $k = 0.0015$. The dissipation, dispersion errors and TMSE are tabulated in Table 1, and we observe that the dispersion error is much greater than the dissipation error. In addition, for $k = 0.0015$ the dispersion error is least when $h = 0.1289$ and greatest when $h = 0.1650$.

From Table 1 and 2, we observe that the errors in W-W-H scheme are higher than those of Z-K scheme. We propose modifications to Z-K scheme with the aim of obtaining better schemes. The first which uses direct local approximation to discretize uu_x term via $u_m^n \delta_x u_m^n$. The resulting finite difference scheme is

$$\frac{u_m^{n+1} - u_m^{n-1}}{2k} + 6u_m^n \left(\frac{u_{m+1}^n - u_{m-1}^n}{2h} \right) + \left(\frac{u_{m+2}^n - 2u_{m+1}^n + 2u_{m-1}^n - u_{m-2}^n}{2h^3} \right) = 0, \qquad (5.3)$$

Table 2: Errors for the schemes at $T = 6$ when $k = 0.0015$ for 1-soliton experiment.

Schemes	h	Dissipation error	Dispersion error	TMSE
Scheme (2.2) Z-K	0.1574	2.2442×10^{-12}	1.6414×10^{-5}	1.6414×10^{-5}
	0.1680	2.4368×10^{-12}	2.2017×10^{-5}	2.2017×10^{-5}
	0.1780	9.2437×10^{-12}	3.5919×10^{-5}	3.5919×10^{-5}
	0.1860	5.7363×10^{-12}	3.4291×10^{-5}	3.4291×10^{-5}
Scheme (2.7) W-W-H	0.1289	5.6542×10^{-11}	6.9921×10^{-5}	6.9921×10^{-5}
	0.1350	9.0535×10^{-11}	8.3456×10^{-5}	8.3456×10^{-5}
	0.1550	3.0882×10^{-10}	1.3739×10^{-4}	1.3739×10^{-4}
	0.1650	3.8986×10^{-10}	1.9170×10^{-4}	1.9170×10^{-4}
Scheme (5.3) NS1	0.1574	8.1498×10^{-12}	5.6540×10^{-5}	5.6540×10^{-5}
	0.1680	1.0879×10^{-11}	7.4858×10^{-5}	7.4858×10^{-5}
	0.1780	3.5624×10^{-11}	1.0949×10^{-4}	1.0949×10^{-4}
	0.1860	2.6794×10^{-11}	1.1507×10^{-4}	1.1507×10^{-4}
Scheme (5.4) NS2	0.1574	3.4778×10^{-12}	2.4079×10^{-5}	2.4079×10^{-5}
	0.1680	3.9517×10^{-12}	3.2134×10^{-5}	3.2134×10^{-5}
	0.1780	1.2636×10^{-11}	5.0381×10^{-5}	5.0381×10^{-5}
	0.1860	9.4637×10^{-12}	4.9777×10^{-5}	4.9777×10^{-5}

and the second which uses central difference for both spatial and time derivative whose nonlinear approximation differs from that of Zabusky-Kruskal scheme. This is given below as

$$\frac{u_m^{n+1} - u_m^{n-1}}{2k} + 6\left(\frac{u_{m+1}^n + 2u_m^n + u_{m-1}^n}{4}\right)\left(\frac{u_{m+1}^n - u_{m-1}^n}{2h}\right) + \left(\frac{u_{m+2}^n - 2u_{m+1}^n + 2u_{m-1}^n - u_{m-2}^n}{2h^3}\right) = 0. \tag{5.4}$$

The amplification factor of the linearized version of the schemes above is given by

$$\xi^2 + I\left\{12\lambda u_{\max}\sin\omega + \frac{\lambda}{h^2}\left(2\sin 2\omega - 4\sin\omega\right)\right\}\xi - 1 = 0, \tag{5.5}$$

which is similar to that of the Z-K scheme. Hence the stability region required for these schemes is

$$\lambda \leq \left|\frac{2}{3\sqrt{3}(2u_{\max} - \frac{1}{h^2})}\right|. \tag{5.6}$$

Following the same arguments as in section 3, we obtain the relative phase error as

$$\text{RPE} = \frac{h^2}{\lambda\omega^3}\tan^{-1}\left\{\frac{\frac{\lambda}{h^2}(2\sin\omega - \sin 2\omega)}{\sqrt{1 - \frac{\lambda^2}{h^4}(\sin 2\omega - 2\sin\omega)^2}}\right\}.$$

Here we highlight the similarities between the linearized scheme for the two NS and Z-K schemes.

The two new schemes NS1 and NS2 are stable for $k = 0.001$ and $k = 0.0015$ in the regions described by the inequalities: $h \geq 0.1358$ and $h \geq 0.1548$ respectively. The tabulated results in Table 1 shows that

the dispersion error is much greater than the dissipation error. We observe that the dispersion error is least when $h = 0.1574$ and greatest when $h = 0.1860$ for $k = 0.0015$.
Figs. 3 and Figs. 4 show the graphs of single soliton solution for the four schemes with a fixed value of h when $k = 0.0015$ at $T = 0$, $T = 3$ and $T = 0$, $T = 6$ respectively, plotted on the same axes. It is seen that as T increases, the wave progresses to the right and at other higher values of T not shown, the waves hit the boundary and appears at the other boundary for all the schemes considered.

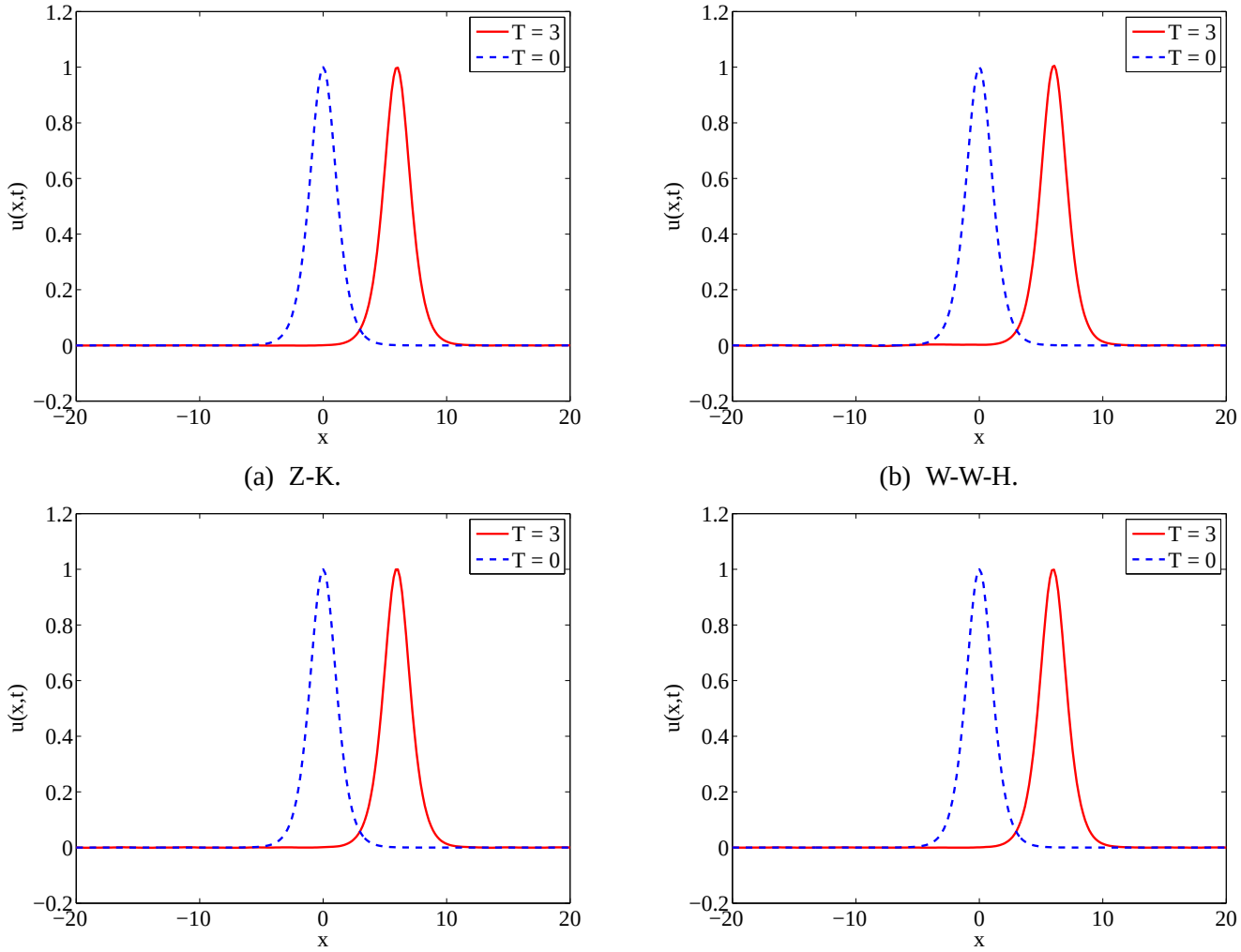

(a) Z-K. (b) W-W-H.

(c) NS1. (d) NS2.

Figure 3: The graph of $u(x,t)$ versus x for single soliton problem for all the schemes with $k = 0.0015$. In (a), (c) and (d), $h = 0.1680$ and in (b) $h = 0.1350$.

In Table 3, we present the errors in the conservation laws. We observe that the errors for the three conservation laws are least at $h = 0.1574$ and greatest when $h = 0.1860$ for Z-K and our proposed schemes but for W-W-H scheme, the least error occurs at $h = 0.1289$ and greatest at $h = 0.1650$.
Figs. 5 shows the graphs of dispersion error versus h and the graphs of the three conservation laws for all the schemes plotted on the same axes for single soliton experiment. Figure 5(a) shows the graph of dispersion error versus h for all the schemes, plotted on the same axes. It is found that the scheme (2.2) has the least dispersion error followed by schemes (5.4), (5.3) and (2.7) respectively. Fig. 5(b) shows the graph of conservation of mass versus h plotted on the same axes for all the schemes. It is observed that schemes

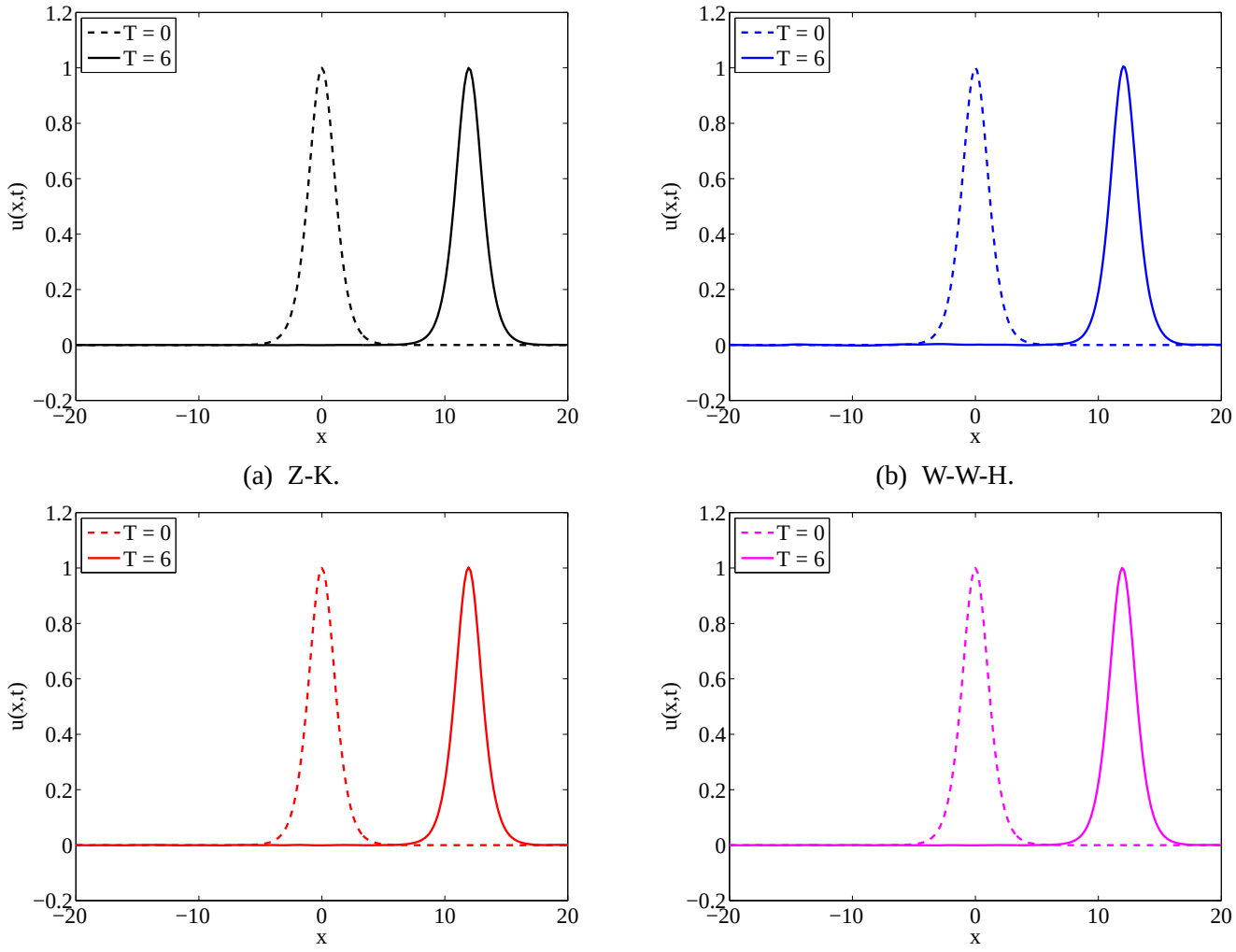

(a) Z-K. (b) W-W-H.

(c) NS1. (d) NS2.

Figure 4: The graph of $u(x,t)$ versus x for single soliton problem for all the schemes with $k = 0.0015$. In (a), (c) and (d), $h = 0.1680$ and in (b) $h = 0.1350$.

(2.2) has the least error of conservation of mass, followed by schemes (5.4), (2.7) and (5.3) respectively. In Fig. 5(c), the graph of conservation of momentum versus h is plotted on the same axes for all the schemes. It is observed that scheme (5.4) has the least error of conservation of momentum, followed by schemes (2.2), (5.3) and (2.7) respectively. The graph of conservation of energy versus h is shown in Fig. 5(d) in which all the schemes are plotted on the same axes. It is seen that scheme (5.4) has the least error of conservation of energy and then followed by schemes (2.2), (5.3) and (2.7) respectively.

In the next experiment we consider the double-soliton problem as follows

Experiment 2

$$\begin{cases} u_t + 6uu_x + u_{xxx} = 0, \ \ \forall\,(x,t) \in (-L,L)\times(0,T), \\ u(x,0) = v(x,0)\,, \\ u(x-L,t) = u(x+L,t). \end{cases} \tag{5.7}$$

Table 3: Conservation laws errors for the schemes at time $T = 3$ when $k = 0.0015$.

Schemes	h	$\|$error $F_1\|$	$\|$error $F_2\|$	$\|$error $F_3\|$	$\max\|u_m - u_m^*\|$
Scheme (2.2)					
Z-K	0.1574	4.5972×10^{-6}	5.1078×10^{-6}	3.0133×10^{-5}	9.2525×10^{-3}
	0.1680	1.7692×10^{-5}	4.5559×10^{-6}	1.9853×10^{-5}	1.0624×10^{-2}
	0.1780	3.6496×10^{-5}	8.2205×10^{-6}	1.1526×10^{-4}	1.3322×10^{-2}
	0.1860	3.4163×10^{-5}	3.4414×10^{-6}	5.3341×10^{-6}	1.3135×10^{-2}
Scheme (2.7)					
W-W-H	0.1289	1.9126×10^{-5}	3.7254×10^{-5}	6.2483×10^{-4}	2.0865×10^{-2}
	0.1350	2.4665×10^{-5}	4.4573×10^{-5}	6.9683×10^{-4}	2.2903×10^{-2}
	0.1550	3.3478×10^{-5}	8.0346×10^{-5}	1.0111×10^{-3}	3.0205×10^{-2}
	0.1650	3.2000×10^{-5}	9.7421×10^{-5}	1.0200×10^{-3}	3.4536×10^{-2}
Scheme (5.3)					
NS1	0.1574	1.4107×10^{-5}	8.8169×10^{-6}	1.7045×10^{-4}	1.6917×10^{-2}
	0.1680	3.8447×10^{-5}	1.0790×10^{-5}	2.0809×10^{-4}	1.9263×10^{-2}
	0.1780	6.9244×10^{-5}	1.7205×10^{-5}	3.6886×10^{-4}	2.3225×10^{-2}
	0.1860	7.0970×10^{-5}	1.5019×10^{-5}	2.7294×10^{-4}	2.3917×10^{-2}
Scheme (5.4)					
NS2	0.1574	6.9832×10^{-6}	2.2598×10^{-6}	2.0455×10^{-5}	1.1151×10^{-2}
	0.1680	2.2921×10^{-5}	1.2105×10^{-6}	3.7724×10^{-5}	1.2749×10^{-2}
	0.1780	4.4749×10^{-5}	8.0677×10^{-6}	1.7943×10^{-4}	1.5774×10^{-2}
	0.1860	4.3456×10^{-5}	1.0472×10^{-6}	6.5158×10^{-5}	1.5800×10^{-2}

where $L = 20$ *and* $v(x,t)$ *is the exact solution given by*

$$v(x,t) = 2(\log f(x,t))_{xx}.$$

with

$$f(x,t) = 1 + e^{\eta_1} + e^{\eta_2} + e^{\eta_1+\eta_2+A_{12}}, \quad \eta_m = \gamma_m x - \gamma_m^3 t + \eta_m^{(0)}, \quad \textit{and} \quad e^{A_{ij}} = \frac{\gamma_i - \gamma_j}{\gamma_i + \gamma_j},$$

see [27]. We also set $T = 3$, $\gamma_1 = 1$, $\gamma_2 = \sqrt{5}$, $\eta_1^{(0)} = 0$ *and* $\eta_2^{(0)} = 10.73$.

Figs. 6 shows the graphs of double soliton solution for the four schemes with a fixed value of h when $k = 0.0015$ at $T = 0$ and $T = 3$, plotted on the same axes. As it is well known, a soliton with larger amplitude has a greater velocity than the smaller one [18]. As T increases, it is observed that the soliton with larger amplitude catches up with that of smaller one(figure not shown). The two soliton waves coalesce for a particular period of time and then separate, still maintaining their original profiles but with change in position. It is also seen that the soliton with the larger amplitude moves ahead of the one with smaller amplitude at $T = 3$. In Figs. 7 when $T = 6$, the wave with larger amplitude hits the wall of the positive boundary and then appears at the negative side of the boundary. This is seen to move towards its original starting point.

For the 2-soliton experiment, Table 4 follows the same trend as in Table 1 and 2 while in Table 5, all the errors are almost the same. Figs. 8 shows the graph of dispersion error versus h and the graphs of the three conservation laws for all the schemes plotted on the same axes for 2-soliton experiment. Fig. 8(a) shows that scheme (2.2) has the least dispersion error, followed by schemes (5.4), (5.3) and (2.7) respectively. Scheme (2.7) has the greatest dispersion error for both single and double soliton experiments. In Fig. 8(b), it is seen

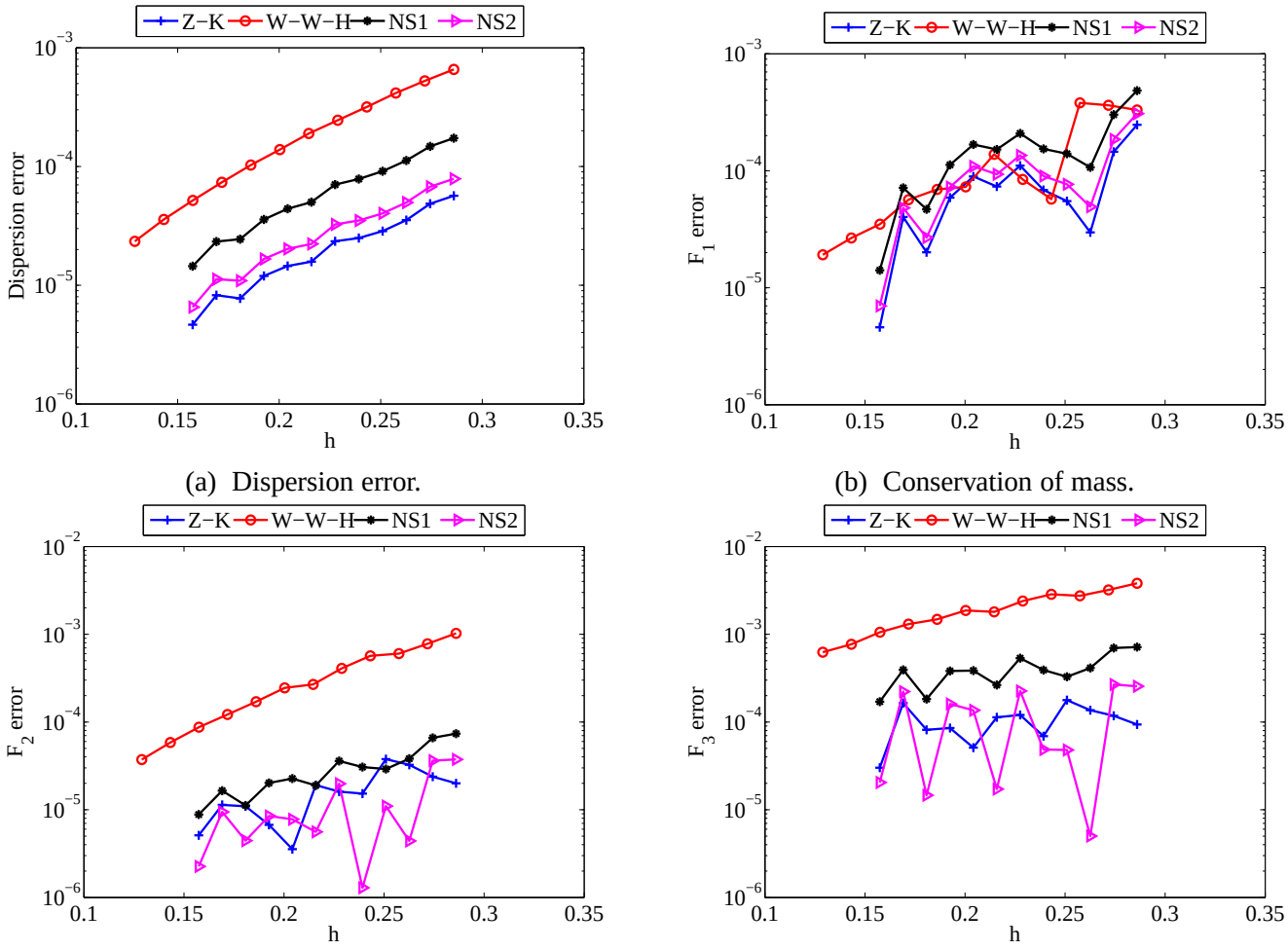

(a) Dispersion error.

(b) Conservation of mass.

(c) Conservation of momentum.

(d) Conservation of energy.

Figure 5: Dispersion error and conservation laws errors for 1-soliton solution for all the schemes at time $T = 3$ when $k = 0.0015$.

that the error of conservation of mass is least for scheme (5.3), followed by schemes (2.2) and (5.4) having almost the same error, while (2.7) has the greatest error. In Figs. 8(c), schemes (2.2) and (5.4) have almost the same error of conservation of momentum which are least, but as h increases beyond a certain point, it is observed that scheme (2.2) becomes better than scheme (5.4). Scheme (5.4) is then followed by (5.3) and (2.7) respectively. In Figs. 8(d), scheme (2.2) has the least error of conservation of energy followed by schemes (5.4), (5.3) and (2.7) respectively.

6 Optimizing parameters for the four schemes

In this section, we aim to compute an optimal value of h which minimizes the dispersion error for a fixed value of k. Based on the results of Experiments 1 and 2, we observe that the dispersion error is much greater than the dissipation error as shown in Table 1 and 4. Hence we follow the same ideas as in the work of [23, 28] to compute the optimal value of h for a given value of k by minimizing the dispersion error. We next describe briefly how various authors use different optimization techniques to determine coefficients of numerical methods, especially designed for Computational Aeroacoustics.

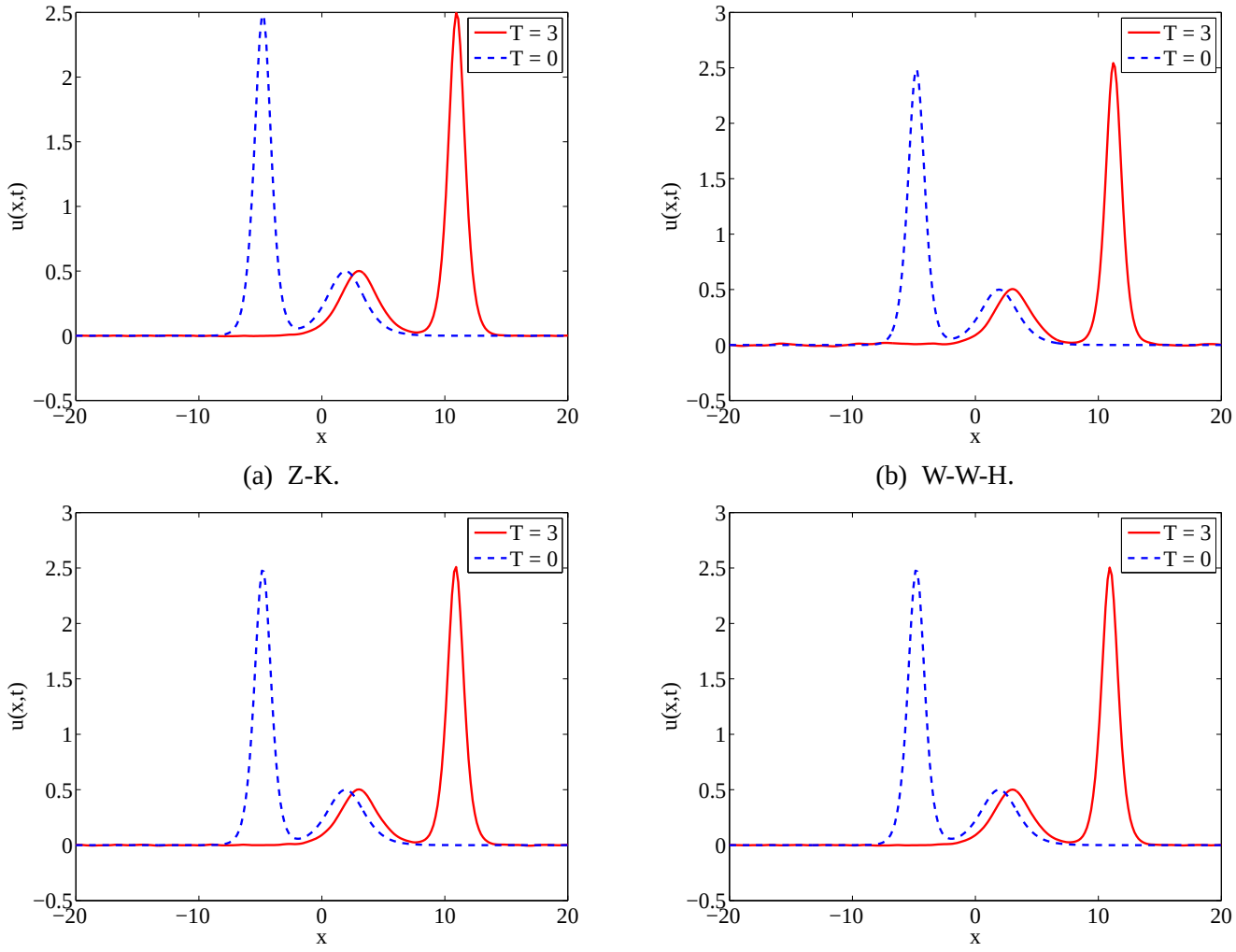

(a) Z-K. (b) W-W-H.

(c) NS1. (d) NS2.

Figure 6: The graph of $u(x,t)$ versus x for double soliton problem for all the schemes at time $T = 3$ with $k = 0.0015$. In (a), (c) and (d), $h = 0.1680$ and in (b) $h = 0.1350$.

Tam and Webb [29] constructed a 7-point and 4th -order central difference method based on the minimization of the dispersion error. They approximated the first order derivative at $x = x_0$ via

$$\frac{\partial u}{\partial x} \approx \frac{1}{h} \sum_{m=-3}^{3} a_m u(x_0 + ih), \tag{6.1}$$

where h is the spacing of a uniform mesh and the coefficients a_m are such that $a_m = -a_{-m}$, providing a scheme without dissipation. On applying spatial Fourier Transform to Eq. (6.1), the numerical wavenumber, θh^* is obtained and is given by

$$\theta h^* = 2 \sum_{m=1}^{3} a_m \sin(m\theta h). \tag{6.2}$$

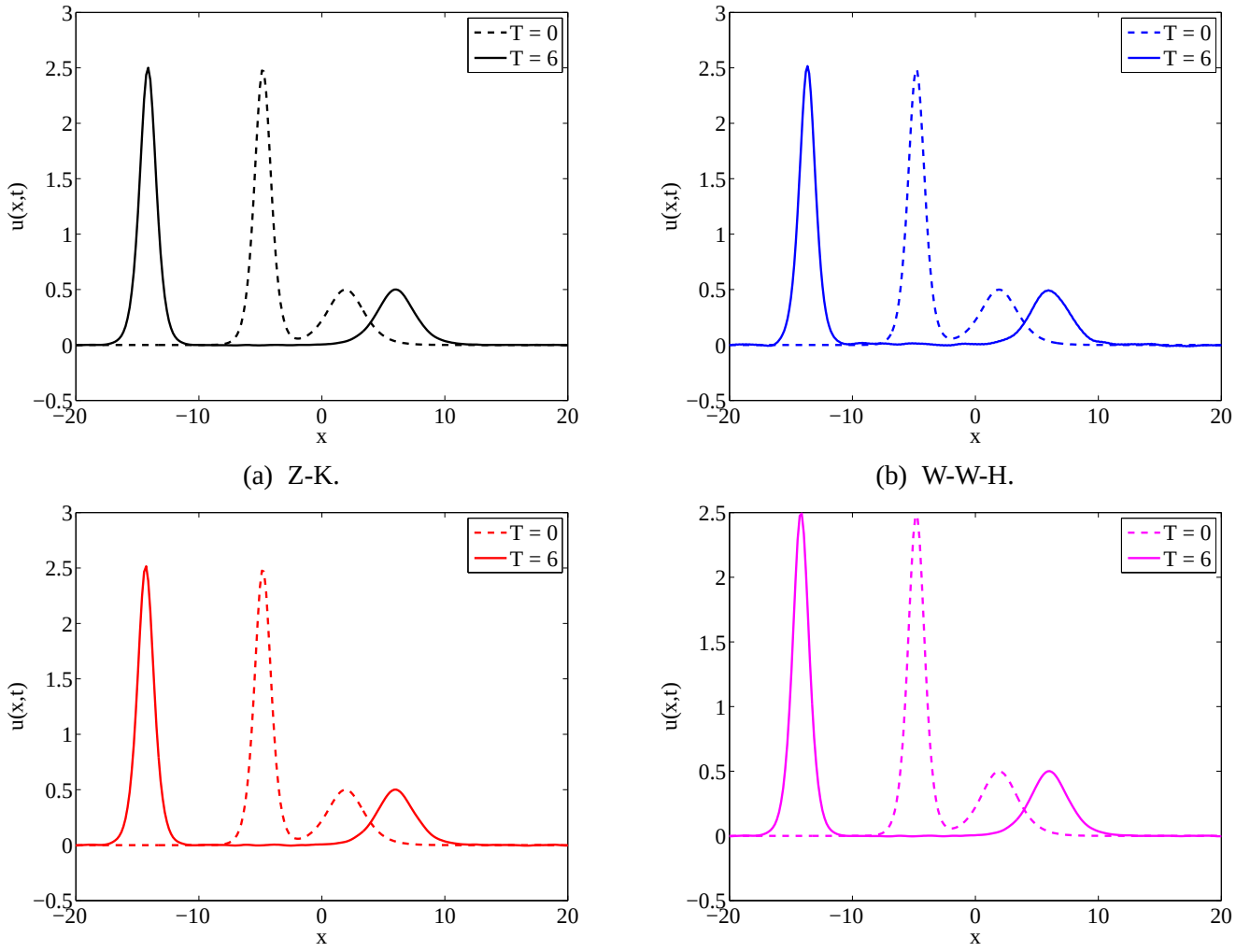

(a) Z-K. (b) W-W-H.

(c) NS1. (d) NS2.

Figure 7: The graph of $u(x,t)$ versus x for double soliton problem for all the schemes at time $T = 3$ with $k = 0.0015$. In (a), (c) and (d), $h = 0.1680$ and in (b) $h = 0.1350$.

Taylor expansion of θh^* from Eq.(6.2) about θh gives

$$2a_1\left(\theta h - \frac{1}{6}(\theta h)^3 + \frac{1}{120}(\theta h)^5\right) + 2a_2\left(2\theta h - \frac{1}{6}(2\theta h)^3 + \frac{1}{120}(2\theta h)^5\right) + 2a_3\left(3\theta h - \frac{1}{6}(3\theta h)^3 + \frac{1}{120}(3\theta h)^5\right) + \cdots \tag{6.3}$$

The 4th-order method is obtained for

$$2a_1 + 4a_2 + 6a_3 = 1$$

$$a_1 + 8a_2 + 27a_3 = 0.$$

Since we have two equations and three unknowns, we can choose, for instance, a_1 as a free parameter. Thus

$$a_2 = \frac{9}{20} - \frac{4}{5}a_1,$$

Table 4: Errors for the schemes at $T = 3$ when $k = 0.0015$ for 2-soliton experiment.

Schemes	h	Dissipation error	Dispersion error	TMSE
Scheme (2.2)				
Z-K	0.1574	1.0818×10^{-10}	1.3690×10^{-3}	1.3690×10^{-3}
	0.1680	1.0546×10^{-10}	1.8114×10^{-3}	1.8114×10^{-3}
	0.1780	9.9928×10^{-11}	2.6563×10^{-3}	2.6563×10^{-3}
	0.1860	1.7882×10^{-10}	2.7841×10^{-3}	2.7841×10^{-3}
Scheme (2.7)				
W-W-H	0.1289	2.5571×10^{-8}	5.3659×10^{-3}	5.3659×10^{-3}
	0.1350	3.8799×10^{-8}	6.4510×10^{-3}	6.4510×10^{-3}
	0.1550	1.2731×10^{-7}	1.1108×10^{-2}	1.1108×10^{-2}
	0.1650	1.9461×10^{-7}	1.5207×10^{-2}	1.5207×10^{-2}
Scheme (5.3)				
NS1	0.1574	3.0535×10^{-9}	4.7940×10^{-3}	4.7940×10^{-3}
	0.1680	3.8099×10^{-9}	6.2848×10^{-3}	6.2848×10^{-3}
	0.1780	6.5723×10^{-9}	8.5919×10^{-3}	8.5919×10^{-3}
	0.1860	7.4545×10^{-9}	9.5599×10^{-3}	9.5599×10^{-3}
Scheme (5.4)				
NS2	0.1574	2.6483×10^{-10}	2.0210×10^{-3}	2.0210×10^{-3}
	0.1680	2.8154×10^{-10}	2.6638×10^{-3}	2.6638×10^{-3}
	0.1780	3.9376×10^{-10}	3.8043×10^{-3}	3.8043×10^{-3}
	0.1860	4.7932×10^{-10}	4.0756×10^{-3}	4.0756×10^{-3}

$$a_3 = \frac{1}{5}\left(a_1 - \frac{2}{3}\right).$$

The numerical wavenumber can be expressed as

$$\theta h^* \approx 2a_1 \sin(\theta h) + 2\left(\frac{9}{20} - \frac{4}{5}a_1\right)\sin(2\theta h) + 2\left(\frac{1}{5}a_1 - \frac{2}{15}\right)\sin(3\theta h).$$

They also defined their integrated error as

$$E = \int_0^{(\theta h)} |\theta h^* - \theta h|^2 \, d(\theta h),$$

where the upper limit of the integral is taken to be $\theta h = 1.1$, since the RPE behaves better in this region [30], to find the value of a_1 which minimizes E. One can then find the values of a_2 and a_3 and thus the approximation for u_x.

Bogey and Bailly [31] minimised the relative difference between the exact phase angle, θh and the numerical phase angle, θh^* and the integrated error is described by

$$E = \int_{\frac{\pi}{16}}^{\frac{\pi}{2}} \frac{|\theta h^* - \theta h|}{\theta h} d(\theta h).$$

Tam [32] summarizes some work in Computational Aeroacoustics. In [23], the author has modified the measures used in [29, 31] in a Computational Aeroacoustic framework to suit them in a case when a numerical scheme is already constructed in the form

$$u_m^{n+1} = \alpha u_{m-1}^n + \beta u_m^n + \gamma u_{m+1}^n. \tag{6.4}$$

Table 5: Errors for the schemes at $T = 6$ when $k = 0.0015$ for 2-soliton experiment.

Schemes	h	Dissipation error	Dispersion error	TMSE
Scheme (2.2) Z-K	0.1574	1.0299×10^{-1}	8.2630×10^{-2}	1.8562×10^{-1}
	0.1680	1.0296×10^{-1}	8.2610×10^{-2}	1.8557×10^{-1}
	0.1780	1.0293×10^{-1}	8.2589×10^{-2}	1.8552×10^{-1}
	0.1860	1.0291×10^{-1}	8.2574×10^{-2}	1.8548×10^{-1}
Scheme (2.7) W-W-H	0.1289	1.0078×10^{-1}	8.1742×10^{-2}	1.8252×10^{-1}
	0.1350	1.0056×10^{-1}	8.1649×10^{-2}	8.2213×10^{-1}
	0.1550	9.9850×10^{-2}	8.1335×10^{-2}	1.8118×10^{-1}
	0.1650	9.9432×10^{-2}	8.1155×10^{-2}	1.8059×10^{-1}
Scheme (5.3) NS1	0.1574	1.0302×10^{-1}	8.2640×10^{-2}	1.8566×10^{-1}
	0.1680	1.0300×10^{-1}	8.2623×10^{-2}	1.8562×10^{-1}
	0.1780	1.0300×10^{-1}	8.2609×10^{-2}	1.8560×10^{-1}
	0.1860	1.0298×10^{-1}	8.2596×10^{-2}	1.8557×10^{-1}
Scheme (5.4) NS2	0.1574	1.0299×10^{-1}	8.2631×10^{-2}	1.8562×10^{-1}
	0.1680	1.0296×10^{-1}	8.2610×10^{-2}	1.8557×10^{-1}
	0.1780	1.0294×10^{-1}	8.2591×10^{-2}	1.8553×10^{-1}
	0.1860	1.0292×10^{-1}	8.2576×10^{-2}	1.8550×10^{-1}

Then appropriate techniques are devised depending on what we want to minimise. For instance, to minimize the dispersion error of the scheme in Eq. (6.4), he defined the following integrals: the Integrated Error from Tam and Webb, (IETAM), and the Integrated Error from Bogey and Bailly, (IEBOGEY). These are defined as follows:

$$\text{IETAM} = \int_0^{1.1} |1 - RPE|^2 d\,\omega, \tag{6.5}$$

$$\text{IEBOGEY} = \int_0^{1.1} |1 - RPE|\, d\omega. \tag{6.6}$$

6.1 Zabusky and Kruskal (1965) scheme

We consider the Z-K scheme given by Eq. (2.2) with $k = 0.0015$ and $u_{max} = 1$. The amplification factor satisfies the equation

$$\xi^2 + I\left\{\frac{0.018}{h}\sin\omega + \frac{0.0015}{h^3}\left(2\sin 2\omega - 4\sin\omega\right)\right\}\xi - 1 = 0, \tag{6.7}$$

and the relative phase error is computed as

$$\text{RPE} = \frac{h^3}{0.0015\omega^3}\tan^{-1}\left\{\frac{\frac{0.0015}{h^3}(2\sin\omega - \sin 2\omega)}{\sqrt{1 - \frac{2.25\times 10^{-6}}{h^6}(\sin 2\omega - 2\sin\omega)^2}}\right\}. \tag{6.8}$$

We compute

$$\text{IETAM} = \int_0^{1.1} (1 - \text{RPE})^2 d\,\omega,$$

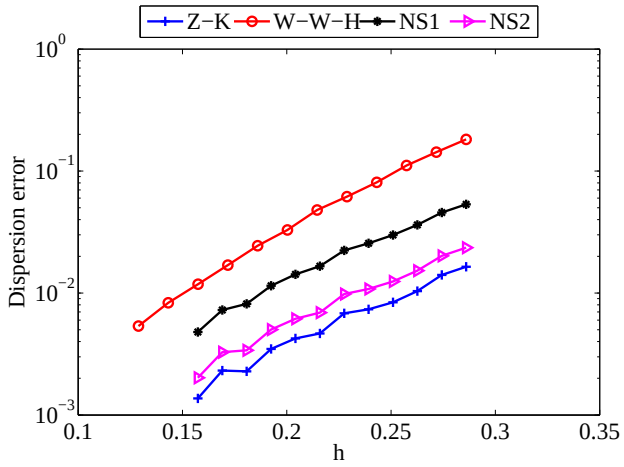

(a) Dispersion error.

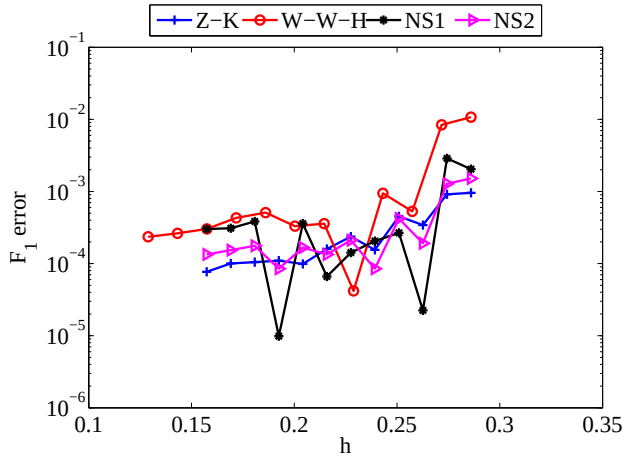

(b) Conservation of mass.

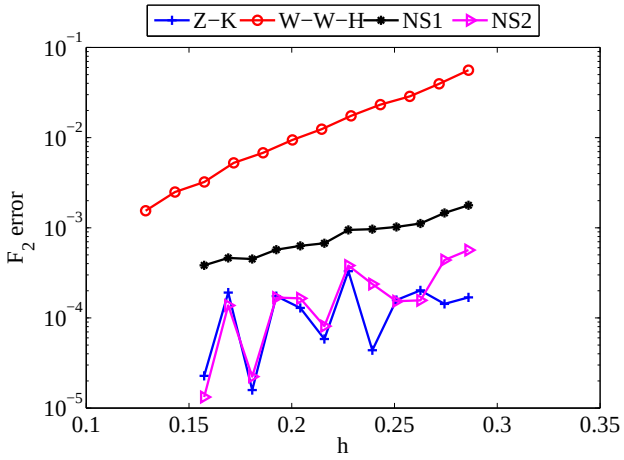

(a) Conservation of momentum.

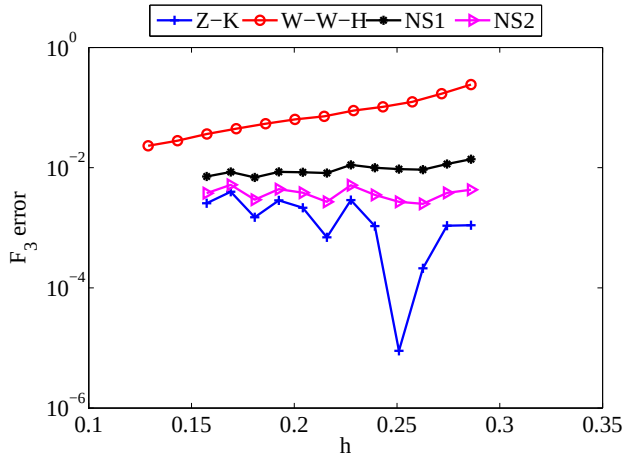

(b) Conservation of energy.

Figure 8: Dispersion error and conservation laws errors for 2-soliton solution for all the schemes at time $T = 3$ when $k = 0.0015$.

which is a function of h. The plot of the integrated error versus h is shown in Fig. 9(a). It is seen that the integrated error increases monotonically with increase in h. Using NLPSolve function in Maple, the optimal h is 0.1574 correct to 4 significant digits.

6.2 Wang et al. (2008) scheme

We consider the W-W-H scheme given by Eq. (2.7) with $k = 0.0015$ and $u_{max} = 1$. The amplification factor of the scheme is

$$(\cos\omega - I\sin\omega)\xi^2 + 2I\sin\omega\left(1 + \frac{0.009}{h} + \frac{0.003}{h^3}(\cos\omega - 1)\right)\xi - (\cos\omega + I\sin\omega) = 0, \qquad (6.9)$$

and the relative phase error is

$$\text{RPE} = \frac{h^3}{0.0015\omega^3}\tan^{-1}\left\{\frac{P\cos\omega + Q\sin\omega}{Q\cos\omega - P\sin\omega}\right\}, \qquad (6.10)$$

where

$$P = -2\sin\omega\left\{1 + \frac{0.003}{h^3}(\cos\omega - 1)\right\}$$

and

$$Q = 2\sqrt{1 - \sin^2\omega\left\{1 + \frac{0.003}{h^3}(\cos\omega - 1)\right\}^2}.$$

The plot of the integrated error versus h shown in Fig. 9(b). It is observed that the integrated error increases monotonically with increase in h. The NLPSolve function in Maple gives an optimal value of h is 0.1289 correct to 4 significant digits.

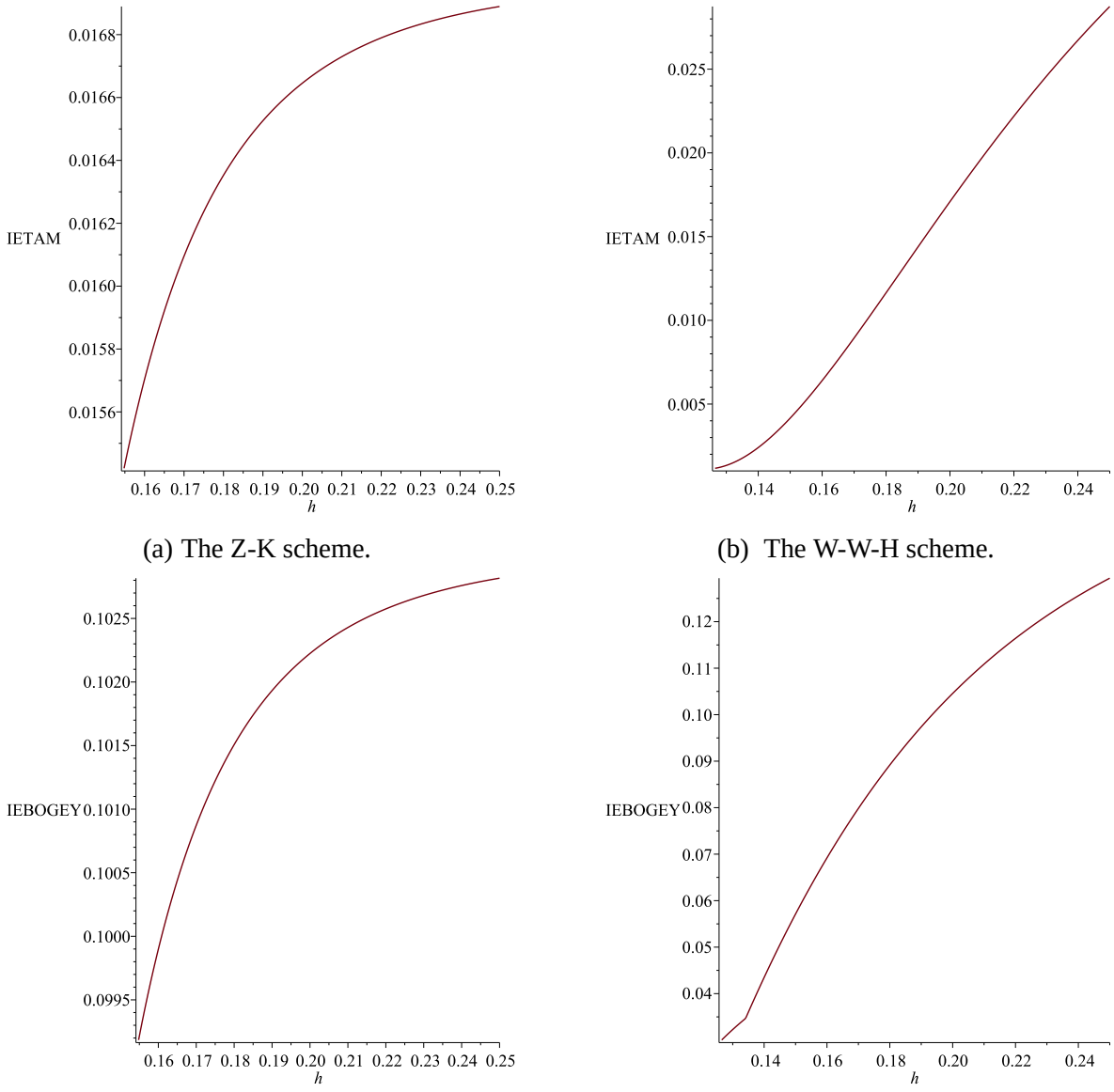

(a) The Z-K scheme.

(b) The W-W-H scheme.

(c) The Z-K scheme.

(d) The W-W-H scheme.

Figure 9: The plot of IETAM and IEBOGEY versus h.

In Figs. 9, it is observed that there is no much difference between the behaviour of IETAM and IEBOGEY

as they are both measures of dispersion error. The IETAM and IEBOGEY for W-W-H scheme are over a larger range when compared with that of Z-K scheme as seen from the graph.

6.3 New schemes

Finally we consider the two new schemes given by Eq. (5.3) and Eq. (5.4) with $k = 0.0015$ and $u_{max} = 1$. The amplification factor and the relative phase error for these schemes are the same as that of Z-K scheme. Hence similar analysis give the optimal h to be 0.1574 correct to 4 significant digits.

6.4 Validation of optimisation process

Next we validate the optimization technique by computing the dispersion error for the two experiments using the optimal values of h. The results are shown in Table 6.

Table 6: Validation of Numerical experiment.

Schemes	Optimal h	Dispersion error for single soliton	Dispersion error for double soliton
Scheme (2.2)			
Z-K	0.1574	4.6514×10^{-6}	1.3690×10^{-3}
Scheme (2.7)			
W-W-H	0.1289	2.3402×10^{-5}	5.3659×10^{-3}
Scheme (5.3)			
NS1	0.1574	1.4464×10^{-5}	4.7940×10^{-3}
Scheme (5.4)			
NS2	0.1574	6.5337×10^{-6}	2.0210×10^{-3}

7 Conclusion

In this work, we have obtained expressions for amplification factor, region of stability and relative phase error for the four schemes considered in solving the 1D KdV equation. Errors are quantified into dissipative and dispersive errors and their ability to conserve the first three integrals is observed. Our two novel schemes are compared with two existing schemes; Z-K scheme and W-W-H scheme. It is found that our schemes and Z-K scheme have the same region of stability which is different from that of W-W-H scheme. We observe that Z-K scheme has the least dispersion error for both the single and double soliton experiments followed by our proposed schemes: (5.4) and (5.3) respectively. W-W-H scheme has the largest dispersion error when compared with other schemes. For 2-soliton experiment, (5.3) conserves mass better than Z-K scheme, but for conservation of momentum, Z-K scheme and scheme (5.4) have almost the same error of conservation of momentum but as h increases, Z-K scheme performs better than others followed by (5.4). For conservation of energy, Z-K scheme performs better than the others followed by schemes (5.4), (5.3) and W-W-H respectively. The results of our numerical experiment are much influenced by the choice of h and k.

The technique of optimisation allows us to compute an optimal value of h at a given value of k. This optimal value of h is validated using numerical experiment. This work can be extended to 2D KdV equation and finite volume methods can be used to solve problems described by KdV equations. The Kadomtsev Petviashvili equation (KP) is a partial differential equation to describe non-linear wave motion that is considered as a generalization of KdV equation to two dimensions.

$$\frac{\partial}{\partial x}\left(\frac{\partial u}{\partial t}+\frac{\partial^3 u}{\partial x^3}+u\frac{\partial u}{\partial x}\right)+\lambda\frac{\partial^2 u}{\partial y^2}=0,$$

$\lambda \neq 1$, $u = u(x, y, t)$: $\mathbb{R}^2 \times \mathbb{R}^+ \to \mathbb{R}$, $t > 0$, $u \in C_1^3$.[33].
Dispersive Riemann problem for KdV equation can also be solved. This problem can be described by

$$u_t + \left(\frac{1}{2}u^2 + \epsilon^2 u_{xx}\right)_x = 0,$$

$$u(x,0) = \begin{cases} u_p, & x < 0 \\ u_r, & x > 0. \end{cases}$$

where $\epsilon^2 << 1$.[34, 35]. Appropriate technique of optimisation can also be used to choose the parameters h and k for minimal numerical dispersion.

Acknowledgements
The authors acknowledge the support of South African DST/NRF SARChI Chair on Mathematical Models and Methods in Bioengineering and Biosciences (M^3B^2) of the University of Pretoria. AR and MC also acknowledge the support of National Research Foundation of South Africa Grant Numbers 95864 and 93476 respectively.

References

[1] D. J. Korteweg and G. de Vries. On the change of form of long waves advancing in a rectangular canal, and on a new type of long stationary waves. *The London, Edinburgh, and Dublin Philosophical Magazine and Journal of Science*, 39(240):422–443, 1895.

[2] A. Ludu, R. A Ionescu, and W. Greiner. Generalized kdv equation for fluid dynamics and quantum algebras. *Foundations of Physics*, 26(5):665–678, 1996.

[3] L. V. Wijngaarden. Linear and non-linear dispersion of pressure pulses in liquid bubble mixtures. In *Proceedings of the 6th Symposium on Naval Hydrodynamics*, 1966.

[4] L. V. Wijngaarden. On the equations of motion for mixtures of liquid and gas bubbles. *Journal of Fluid Mechanics*, 33(03):465–474, 1968.

[5] M. D. Kruskal. *Asymptotology in numerical computation: Progress and plans on the Fermi-Pasta-Ulam problem*. Princeton University Plasma Physics Laboratory, 1966.

[6] N. J. Zabusky. A synergetic approach to problems of nonlinear dispersive wave propagation and interaction. In *Proc. Symp. Nonlinear Partial Differential Equations, Editor W. Ames, New York, Academic Press*, pages 223–258, 1967.

[7] C. S. Gardner and G. K. Morikawa. Similarity in the asymptotic behavior of collision-free hydromagnetic waves and water waves. Technical report, New York Univ., New York. Inst. of Mathematical Sciences, 1960.

[8] H. Washimi and T. Taniuti. Propagation of ion-acoustic solitary waves of small amplitude. *Physical Review Letters*, 17(19):996, 1966.

[9] A. C. Vliegenthart. On finite-difference methods for the Korteweg-de-Vries equation. *Journal of Engineering Mathematics*, 5(2):137–155, 1971.

[10] H. Wang, Y. Wang, and Y. Hu. An explicit scheme for the Korteweg-de-Vries equation. *Chinese Physics Letters*, 25(7):2335–2338, 2008.

[11] N. J. Zabusky and M. D. Kruskal. Interaction of solitons in a collisionless plasma and the recurrence of initial states. *Physical Review Letters*, 15(6):240–243, 1965.

[12] K. Djidjeli, W. G. Price, E. H. Twizell, and Y. Wang. Numerical methods for the solution of the third-and fifth-order dispersive Korteweg-de-Vries equations. *Journal of Computational and Applied Mathematics*, 58(3):307–336, 1995.

[13] U. M. Ascher and R. I. McLachlan. On symplectic and multisymplectic schemes for the Korteweg-de-Vries equation. *Journal of Scientific Computing*, 25(1):83–104, 2005.

[14] B. A. Refik. Exponential finite-difference method applied to Korteweg-de-Vries equation for small times. *Applied Mathematics and Computation*, 160(3):675–682, 2005.

[15] M. C. Bhattacharya. An explicit conditionally stable finite difference equation for-heat conduction problems. *International Journal for Numerical Methods in Engineering*, 21(2):239–265, 1985.

[16] L. L. Takacs. A two-step scheme for the advection equation with minimized dissipation and dispersion errors. *Monthly Weather Review*, 113(6):1050–1065, 1985.

[17] J. C. Strikwerda. *Finite difference schemes and partial differential equations*. Society for Indistrial and Applied Mathematics. Philadelphia. Second edition., 2004.

[18] I. T. Greig and J. L. Morris. A hopscotch method for the Korteweg-de-Vries equation. *Journal of Computational Physics*, 20(1):64–80, 1976.

[19] J. J. H. Miller. On the location of zeros of certain classes of polynomials with applications to numerical analysis. *IMA Journal of Applied Mathematics*, 8(3):397–406, 1971.

[20] T. W. H. Sheu, S. K. Wang, and R.K. Lin. An implicit scheme for solving the convection–diffusion–reaction equation in two dimensions. *Journal of Computational Physics*, 164(1):123–142, 2000.

[21] C. Hirsch. *Numerical computation of internal and external flows*. John Wiley & Sons. Vol 2., 1990.

[22] A. R. Appadu and M. Z. Dauhoo. The concept of minimized integrated exponential error for low dispersion and low dissipation schemes. *International Journal for Numerical Methods in Fluids*, 65(5):578–601, 2011.

[23] A. R. Appadu. Comparison of some optimisation techniques for numerical schemes discretising equations with advection terms. *International Journal of Innovative Computing and Applications*, 4(1):12–27, 2012.

[24] A. R. Appadu. Some applications of the concept of minimized integrated exponential error for low dispersion and low dissipation. *International Journal for Numerical Methods in Fluids*, 68(2):244–268, 2012.

[25] A. R. Appadu. The technique of mieeldld in computational aeroacoustics. *Journal of Applied Mathematics*, 2012, 2012.

[26] K. Brauer. The Korteweg-de-Vries equation: History, exact solutions, and graphical representation. *Germa ny University of Osnabrueck*, 2000.

[27] T. R. Taha and M. I. Ablowitz. Analytical and numerical aspects of certain nonlinear evolution equations. iii. numerical, Korteweg-de-Vries equation. *Journal of Computational Physics*, 55(2):231–253, 1984.

[28] A. R. Appadu. Numerical solution of the 1d advection-diffusion equation using standard and nonstandard finite difference schemes. *Journal of Applied Mathematics*, 2013, 2013.

[29] C. K. Tam and J. C. Webb. Dispersion-relation-preserving finite difference schemes for computational acoustics. *Journal of Computational Physics*, 107(2):262–281, 1993.

[30] C. K. Tam and H. Shen. Direct computation of nonlinear acoustic pulses using high order finite difference schemes. *AIAA Paper*, 4325:1993, 1993.

[31] C. Bogey and C. Bailly. A family of low dispersive and low dissipative explicit schemes for flow and noise computations. *Journal of Computational Physics*, 194(1):194–214, 2004.

[32] C. K. Tam. Computational aeroacoustics: an overview of computational challenges and applications. *International Journal of Computational Fluid Dynamics*, 18(6):547–567, 2004.

[33] Gomez E. Lopez W. Sajo A. Arvelo, L. and C. Vega. Numerical solution of KdV and KP equations by using finite difference compact schemes. *CIMPA*, 2012.

[34] D Zeidan. The Riemann problem for a hyperbolic model of two-phase flow in conservative form. *International Journal of Computational Fluid Dynamics*, 25(6):299–318, 2011.

[35] E. F. Toro. *Riemann solvers and numerical methods for fluid dynamics: A practical introduction*. Springer. Third edition, 1999.